HARMONIA | COST ACTION 21119

Virtual Mobility Grant

ASSESSING THE ACCURACY, UNCERTAINTY AND SPATIOTEMPORAL RESOLUTION OF SPACE-BORN AEROSOL INDEX PRODUCTS ON GEOSTATIONARY AND POLAR ORBITS.

Panagiotis Fountoukidis

Laboratory of Atmospheric Physics, Aristotle University of Thessaloniki, Greece

TABLE OF CONTENTS

LIST OF FIGURES

LIST OF TABLES

1. Introduction

This VM contributes to the COST Action objective *T3.3: Investigate and report on the role of aerosol uncertainty on user requirements*, as well as the deliverable *D3.2 Report on the requirements of different user communities on the accuracy, uncertainty and spatiotemporal resolution of aerosol measurements needed for their activities*.

The main object of the VM was the evaluation of the Absorbing Aerosol Index (AAI), or UV Aerosol Index (UVAI), derived from the South Korean GEMS/KOMPSAT-2B (Geostationary Environment Monitoring Spectrometer/KOrea Multi-Purpose SATellite-2B) satellite against S5P/TROPOMI and GOME-2 B&C AAI products, on Low Earth Orbits (LEO). The aerosol index, being a non-geophysical parameter, cannot offer accuracy levels, it is however used by the space-born Aerosol Layer Height (ALH) algorithms, either as a trigger to initialise the ALH retrieval, or as a flag to mask the ALH data. The ALH is a focal satellite-based observational dataset for assimilation by the ECMWF atmospheric forecasting, and hence its importance in providing timely and consolidated information on air quality to decision makers quite relevant. By assessing the AI, we are indirectly ensuring that the ALH dataset is optimised and offering the best possible understanding on the transport and loft of aerosols on a continental scale.

1.1 Reference Documents

The following documents are referenced in this document. They have been used (in the sense of tailoring) to prepare the document on hand.

Table 1-1. Reference Documents

Title		Document ID	Issue
[RD01]	GEMS Algorithm Theoretical Basis Document, Aerosol Retrieval Algorithm	Provided by private communication, not available on the GEMS website. [V1.1 from April 2020 is available online: https://nesc.nier.go.kr/en/html/satellite/doc/doc.do]	Version 2.0 20/12/2022
[RD02]	Algorithm Theoretical Basis Document for the NRT, Offline and Data Record Absorbing Aerosol Index Products	ACSAF/KNMI/ATBD/002	2.70
[RD03]	NRT and Offline GOME-2C Absorbing Aerosol Index product	SAF/AC/KNMI/VR/007	1/2019
[RD04]	Product User Manual for the NRT, Offline and Data Record Absorbing Aerosol Index Products (GOME-2)	ACSAF/KNMI/PUM/002	1.90
[RD05]	Quarterly Validation Report of the Copernicus Sentinel-5 Precursor Operational Data Products #16: April 2018 – August 2022	S5P-MPC-IASB-ROCVR-16.01.00-20220923	16.01.00
[RD06]	Reprocessed GOME-2 Absorbing Aerosol Index product	SAF/O3M/KNMI/VR/003	2/2016
[RD07]	Sentinel-5 precursor/TROPOMI Level-2 Product User Manual UV Aerosol Index	S5P-KNMI-L2-0026-MA	2.4.0
[RD08]	TROPOMI ATBD of the UV aerosol index	S5P-KNMI-L2-0008-RP	2.1.0
[RD09]	Product User Manual, GOME-2 Absorbing Aerosol Height	SAF/AC/KNMI/PUM/006	1.2
[RD10]	SAF Validation Report, Absorbing Aerosol Height products	SAF/AC/AUTH-RMI/VR/001	1/2020

2. Executive Summary

In this VM we present the evaluation of the Absorbing Aerosol Index (AAI), or UV Aerosol Index (UVAI), derived from the South Korean GEMS/KOMPSAT-2B (Geostationary Environment Monitoring Spectrometer/KOrea Multi-Purpose SATellite-2B) satellite against S5P/TROPOMI and GOME-2 B&C AAI products, on Low Earth Orbits (LEO). The comparisons focused on specific dust events over Asia during the period January 2023 to May 2024. To permit the satellite-to-satellite comparisons, L3 AI products from the three sensors in 0.5^o x 0.5^o grid were performed, enabling the calculation of collocated absolute differences between the reference and the GEMS L3 datasets. From this analysis it was found that the GEMS AAI product shows an overestimation compared to S5P-TROPOMI and GOME-2 B/C. This overestimation is demonstrated below by a satellite-to-satellite comparisons which are presented for selected case studies. A general overview of this analysis is that the AAI is strongly connected to the event and or the sensor. This in practice means the comparative results can be different depending on the events that were analysed.

Furthermore, we demonstrate the effect that the calculation of the aerosol index has on the assessment of the Aerosol Layer Height, an important parameter for both air quality as well as climate studies. This product is relatively new both in the LEO as well as the GEO satellite remote sensing communities and heavily depends on the AI levels, as well as the Aerosol Optical Depth retrieved simultaneously by the individual space-born aerosol algorithms.

3. Data and methodology

3.1 GEMS L2 UV Aerosol Index v2.0 dataset

The Korean geostationary environmental satellite (GEMS) was launched in February 2020 to monitor air quality over Asia. GEMS is one of the global constellation instruments that observes air quality (Kim et al., 2019). Details on the platform and instrument may be seen in **Table 3-2**. The field of views (FOV) of the GEMS are shown in **Figure 3-1** while the availability of the GEMS observations depending on sensing time and season is provided in **Table 3-1.**

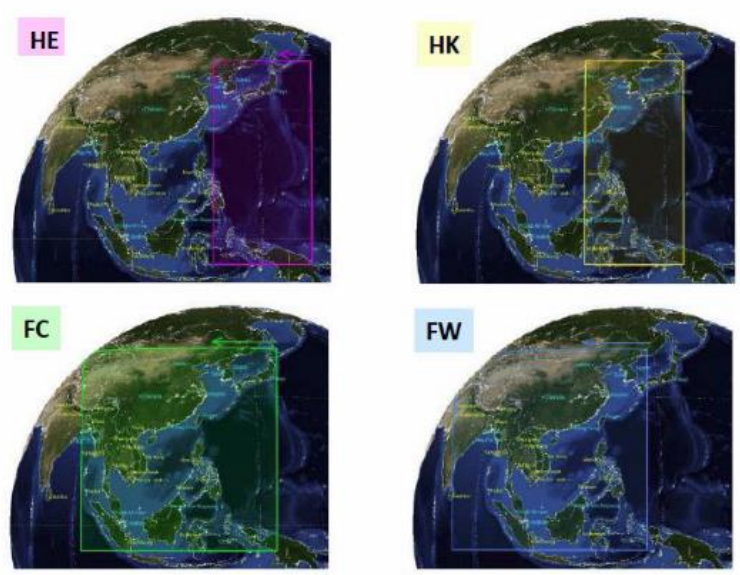

Figure 3-1. The scan geometries of the GEMS instrument, where HE denotes Half East, HK Half Korea, FC Full Central and FW Full West.

Table 3-1. GEMS data availability per hour 1 availability per hour of observation depending on season for the different scan geometries of GEMS

UTC	23:00	0:00	1:00	2:00	3:00	4:00	5:00	6:00	7:00	8:00
Jan	X	X	HE	HK	FC	FW	FW	FW	X	X
Feb	X	X	HE	HK	FC	FW	FW	FW	FW	X
Mar	X	HE	HK	FC	FC	FW	FW	FW	FW	X
Apr	HE	HK	FC	FC	FC	FW	FW	FW	FW	FW
May	HE	HK	FC	FC	FW	FW	FW	FW	FW	FW
Jun	HE	HK	FC	FC	FW	FW	FW	FW	FW	FW
Jul	HE	HK	FC	FC	FW	FW	FW	FW	FW	FW
Aug	HE	HK	FC	FC	FW	FW	FW	FW	FW	FW
Sep	HE	HK	FC	FC	FW	FW	FW	FW	FW	FW
Oct	X	HE	HK	FC	FC	FW	FW	FW	FW	X
Nov	X	X	HE	HK	FC	FW	FW	FW	X	X
Dec	X	X	HE	HK	FC	FW	FW	FW	X	X

L2 GEMS v2.0 Aerosol datasets (Aerosol Layer Height and UV Aerosol Index) up to May 2024 have been used for this assessment, as follows.

For the GEMS instrument, the Ultra-Violet Aerosol Index (UVAI) is retrieved via an aerosol retrieval algorithm. The main products of this algorithm are the Aerosol Optical Depth (AOD) and the Single Scattering Albedo (SSA). The main assumption of the algorithm is that the measured spectrum consists of wavelength-dependent Rayleigh scattering and aerosol effects, where the aerosol information can be retrieved by fitting the spectrum. Thus, to retrieve the above mentioned two products, a Look-Up Table (LUT) approach and an Optimal Estimation (OE) method is applied. In addition, to achieve better accuracy of the retrievals, the Aerosol Layer Height (ALH) is retrieved from the algorithm, as well. Before retrieving the Aerosol Index (AI), all cloudy pixels are removed, and the surface reflectance is corrected using the Ozone Monitoring Instrument Lambertian Equivalent Reflectance (OMI LER) dataset **[RD01]**.

The AI can be retrieved from measurements in either UV, or Visible solar spectrum. The UVAI is a strong indicator for the presence of absorbing aerosols, while the Visible AI can provide us information about the optical depth and the size of the aerosols. To retrieve the UV and Visible AI, two pairs of wavelengths are used, 354-388 nm and 477-490 nm, respectively. On this report, as AI we will refer to the UVAI, or the Absorbing Aerosol Index (AAI).

In general, the AI is defined as:

$$\text{AI} = -100\left[log\left(\frac{N_{\lambda 1}}{N_{\lambda 2}}\right)_{meas} - log\left(\frac{N_{\lambda 1}(LER_{\lambda 1})}{N_{\lambda 2}(LER_{\lambda 2})}\right)_{calc}\right] \qquad (1)$$

where, $N_{\lambda 2}$ and $N_{\lambda 1}$ are the normalized radiances, at the two wavelengths ($\lambda_2 > \lambda_1$), the subscripts *meas* and *calc* represent the measured and calculated radiances, respectively, and LER indicates the surface reflectance estimated by correcting Rayleigh scattering under the aerosol-free assumption **[RD01]**.

3.2 S5P/TROPOMI and GOME2/MetopB & C Aerosol Index datasets

The main characteristics of the satellite instruments used in this evaluation are summarized in **Table 3-2**.

Table 3-2. Main characteristics of the GEMS, S5P/TROPOMI and GOME2/MetopB & C instruments.

	GEMS	TROPOMI	GOME2
Platform	GEO-KOMPSAT-2B	Sentinel 5-P	MetOp-B, C
Principle	Geostationary Spectrometer	Polar orbit push broom grating spectrometer	Polar orbit grating spectrometer

Spatial resolution	3.5 x 8 km^2	5.5× 3.5 km^2	80 x 40 km^2
Coverage	5°S - 45°N, 75°E - 145°E	Global coverage every day, in daylight	Global coverage every 3 days, in daylight
Swath width	5000 km	2600 km	1920 km
Spectral range	300 - 500 nm	270–495 nm, 675–775 nm, 2305–2385 nm	240-315 nm, 311-403 nm, 401-600 nm, 590-790 nm
Eq. crossing time	Geostationary	13:30 LT	09:30 LT

The main satellite instruments used in the evaluation of the GEMS aerosol products are:

- The TROPOspheric Monitoring Instrument (TROPOMI) is a nadir viewing shortwave spectrometer, which uses passive remote sensing techniques. TROPOMI measures in three wavelength ranges, the UV-Visible wavelength range (270 – 500 nm), the near infrared range (710 – 770 nm) and the shortwave infrared range (2314 – 2382 nm). It is part of the Sentinel-5 Precursor (S5P) mission, which is a Low Earth Orbit (LEO) polar satellite. S5P was launched successfully on 13 October 2017
- The Global Ozone Monitoring Experiment-2 (GOME-2) Meteorological Operational satellite (MetOp) B/C is a nadir viewing across-track scanning spectrometer, which measures the radiance back-scattered from the atmosphere and the surface of the Earth in the ultraviolet and visible range (200 – 790 nm). GOME-2 is part of the MetOp satellites, which are in polar orbit around the Earth.

The main datasets used in the evaluation of the GEMS aerosol products are:

- **The TROPOMI *aerosol_index_354_388*.** In TROPOMI, the UVAI is calculated via the satellite measured Earth radiance and pre-computed LUT values (e.g., surface reflectance, spherical albedo of the atmosphere). To derive the AI, the assumption of a LER surface and that the LER surface is assumed to be equal at both wavelengths, are made **[RD08]**. S5P/TROPOMI UVAI has been validated using the UVAI products from the Earth Observing System Aura Ozone Monitoring Instrument (EOS-Aura OMI) and the Suomi National Polar-orbiting Partnership Ozone Mapping and Profiler Suite (Suomi-NPP OMPS) **[RD05]**. From these comparisons a mean bias of –0.8990 between S5P UVAI and OMPS UVAI was found. Currently, with the latest versions of the product, UVAI is compliant to bias requirements with a global mean average close to –0.5 UVAI units **[RD05]**.

- **The GOME2/MetopB-C *AAI* at *340-380nm***. In GOME-2 B/C, the AI product refers to the joint product of AAI and SCI (Scattering Index) as residue. The calculation of the residue is based on the reflectance at the top of the atmosphere (using the measured radiance at the top of the atmosphere) and the reflectance assuming a molecular atmosphere. These parameters are calculated with a LUT approach, for various atmospheric conditions (SZA, surface albedo, ozone column) **[RD02]**. The GOME-2B UVAI product was compared to the SCanning Imaging Absorption spectroMeter for Atmospheric CartograpHY (SCIAMACHY) AAI, for several case studies during 2007 and 2008 **[RD06]**. For a specific day (2008-07-13), the results showed a good correlation between the two products (slope = 1.07 ± 0.06, intercept = –0.01 ± 0.05) **[RD06]**. The GOME-2C UVAI was compared to the S5P/TROPOMI UVAI, for specific dust events (2019-05-20 and 2019-09-11) **[RD03]**. In both of these case studies, a good agreement of the geophysical patterns between the two products was reported based on map representations. However, the absolute levels of the TROPOMI UVAI product were lower when compared to the GOME-2C UVAI **[RD03]**.

3.3 Quality assurance of the Aerosol Index datasets

The recommended quality flags have been applied, according to the instructions provided by the relative ATBD and PUM files for all four satellite datasets.

For the **S5P-TROPOMI L2 AI** product we set the quality flag parameter *qa_value* to be greater than 0.8 (*qa_value* > 0.8) **[RD07]**. In addition, after personal communication with the data providers and in-house investigations, we applied one extra quality flag on the product:

- The eastern-most pixels were excluded, i.e. we only accepted pixels at row positions ≤ 400

For the **GOME-2 MetOp B/C L2 AI**, according to the information of the PUM file, we applied the following quality flags **[RD04]**:

- cloud fraction < 0.2 (*PMD_CloudFraction* parameter)
- sun glint = 0, no sun glint effect (*SunGlintFlag* parameter)
- scattering angle > 90 (*ScatteringAngle* parameter)
- scan direction = 1, keep only the forward scans (*ScanDirection* parameter)

For the **v1.0 and v2.0 GEMS L2 UVAI** product, the following quality flags have been applied, after personal communication with the data providers:

- keep only the land (*GroundPixelQualityFlags* parameter)
- no sunglint effect (*GroundPixelQualityFlags* parameter)
- keep only the snow/ice free regions (*GroundPixelQualityFlags* parameter)
- keep the reliable data (*FinalAlgorithmFlags* parameter)
- cloud masking (*FinalAlgorithmFlags* parameter)
- sun glint angle > 35^o (*FinalAlgorithmFlags* parameter)
- sza < 60^o (*SolarZenithAngle* parameter)

3.4 Evaluation approach

For the evaluation of the GEMS L2 UVAI product, a comparison between the GEMS AI and three other reference satellite AI L2 products (S5P-TROPOMI and GOME-2 B/C) was conducted. Satellite-to-satellite comparisons between the three AI products are presented, for specific dust events over Asia, during 2024. For those comparisons, the L3 AAI (0.5^o x 0.5^o) data were calculated for all three sensors. The results are presented via scatter plots and box plots of the absolute difference between the reference and the GEMS L3 data.

In the context of this report, map representations over Asia were made aiming to check the three instruments' ability to capture the same aerosol load. Specific dates of intense dust events over E. Asia, during March 2021, were selected. These maps were used to demonstrate, as well as to investigate, the effect of the proposed GEMS flagging system and provide the first assessment of the dataset. To reduce the influence of the different resolutions all data sets were hence gridded. In addition, for the comparison of the aerosol retrievals the different observation times were considered. For each overpass of a polar orbiting satellite, we used the closest temporal GEMS scandisk.

4. Aerosol Index Evaluation

Several dust events in Asia were identified during the GEMS sensing period 2020 to 2024 and most of them started from the Gobi Desert and spread aerosol through the continent. Two case studies within spring 2024 will only be shown here, for brevity reasons. To conduct a quantitative comparison, we focused on a specific region where mostly absorbing aerosols can be found from the Gobi Desert to the Korean Peninsula (33º-45ºN and 75 º-135ºE).

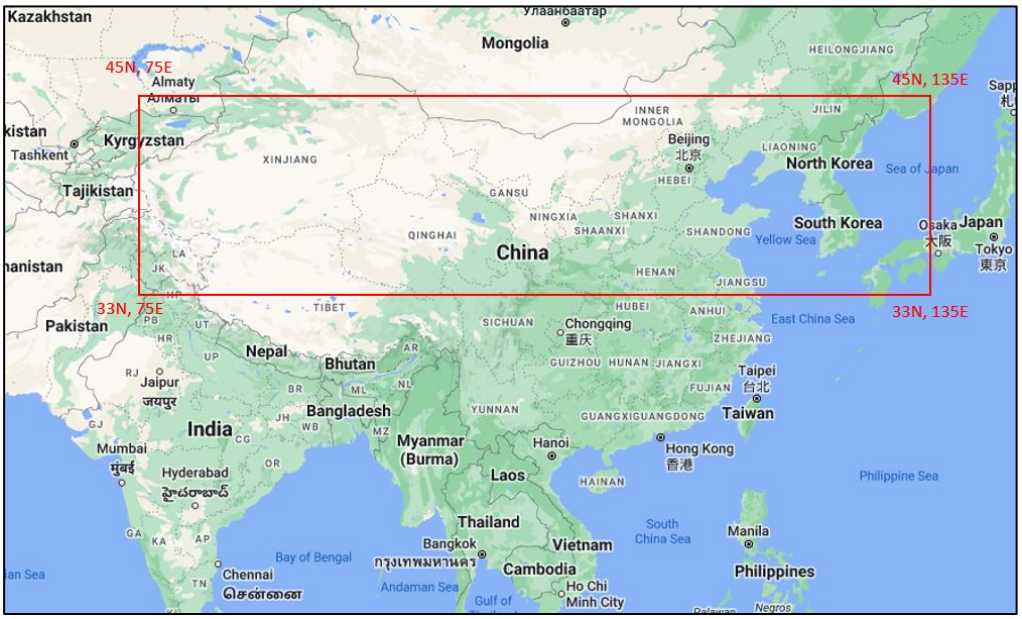

Figure 4-1. The area of interest (Gobi Desert and the Korean Peninsula)

For those pixel-to-pixel comparisons, we converted the L2 AAI products into L3 (0.5° x 0.5° gridded data). For the GEMS v2.0 AAI dataset, we used the observational times closer to the S5P-TROPOMI and GOME-2 B & C overpasses through Asia. Thus, for S5P-TROPOMI we used the GEMS times 03:45, 04:45 and 05:45 UTC and for GOME-2 B & C we used the times 00:45, 01:45 and 02:45 UTC.

4.1 Case study | March 21, 2023

A large dust storm affected air quality over central Asia on March 21st, 2023, shown via the GEMS AI product in Figure 4-2, left. The comparison of this product against collocated L3 data from S5P/TROPOMI, on a LEO orbit, in the same figure on the right, shows a promising agreement in the case of strong dust events, with an R^2 of 0.71, a slope of near unity and a systematic overestimation by GEMS of 0.4.

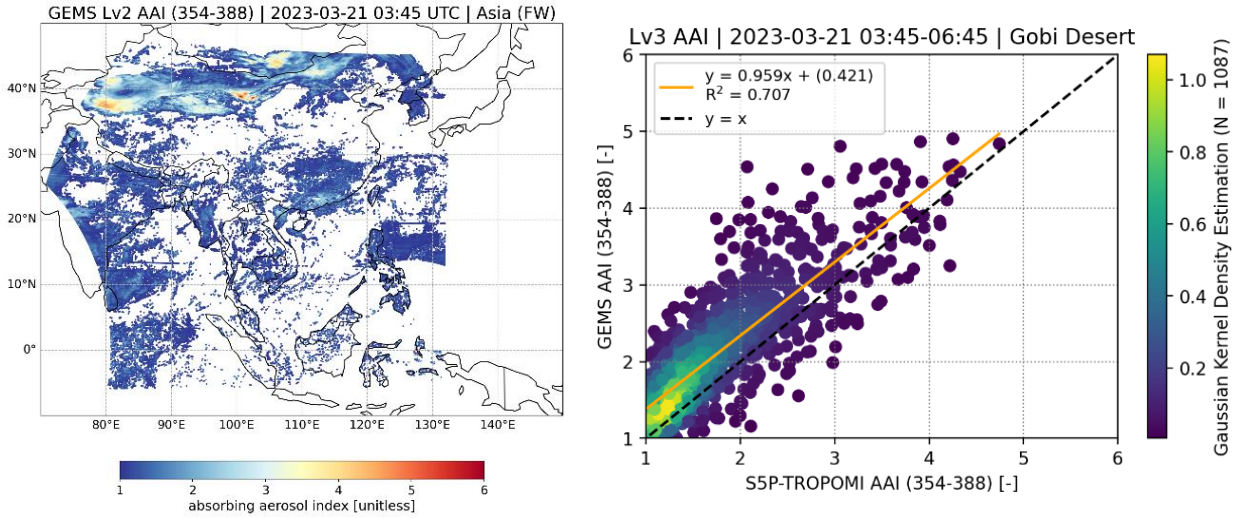

Figure 4-2. (left) the Aerosol Index over the entire GEMS field of regard (right) scatter plot of the L3 spatiotemporal collocated AAI between GEMS and S5P/TROPOMI on March 21. 2023.

4.2 Case study | March 27, 2024

The case study of March 27, 2024 (Figure 4-3), is one of the main cases that was analyzed, and the results are presented in this report. The comparison results between the GEMS and the reference datasets (S5P/TROPOMI and GOME-2 B&C) are presented as scatter plots and box plots of the absolute differences between the reference datasets and the GEMS (**Figure 4-4**).

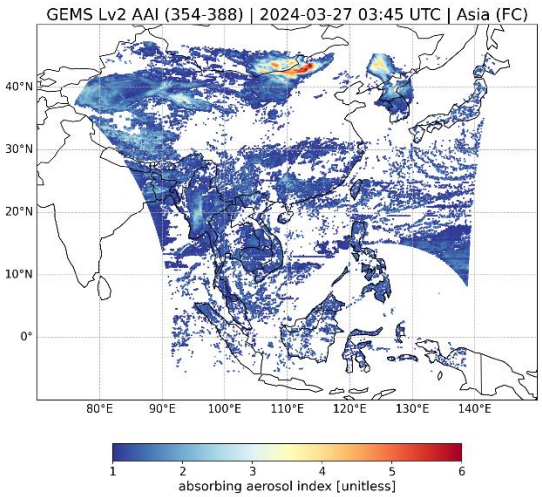

Figure 4-3. The strong dust event on March 27th, 2024, analysed in this work as shown by the GEMS L2 AI product.

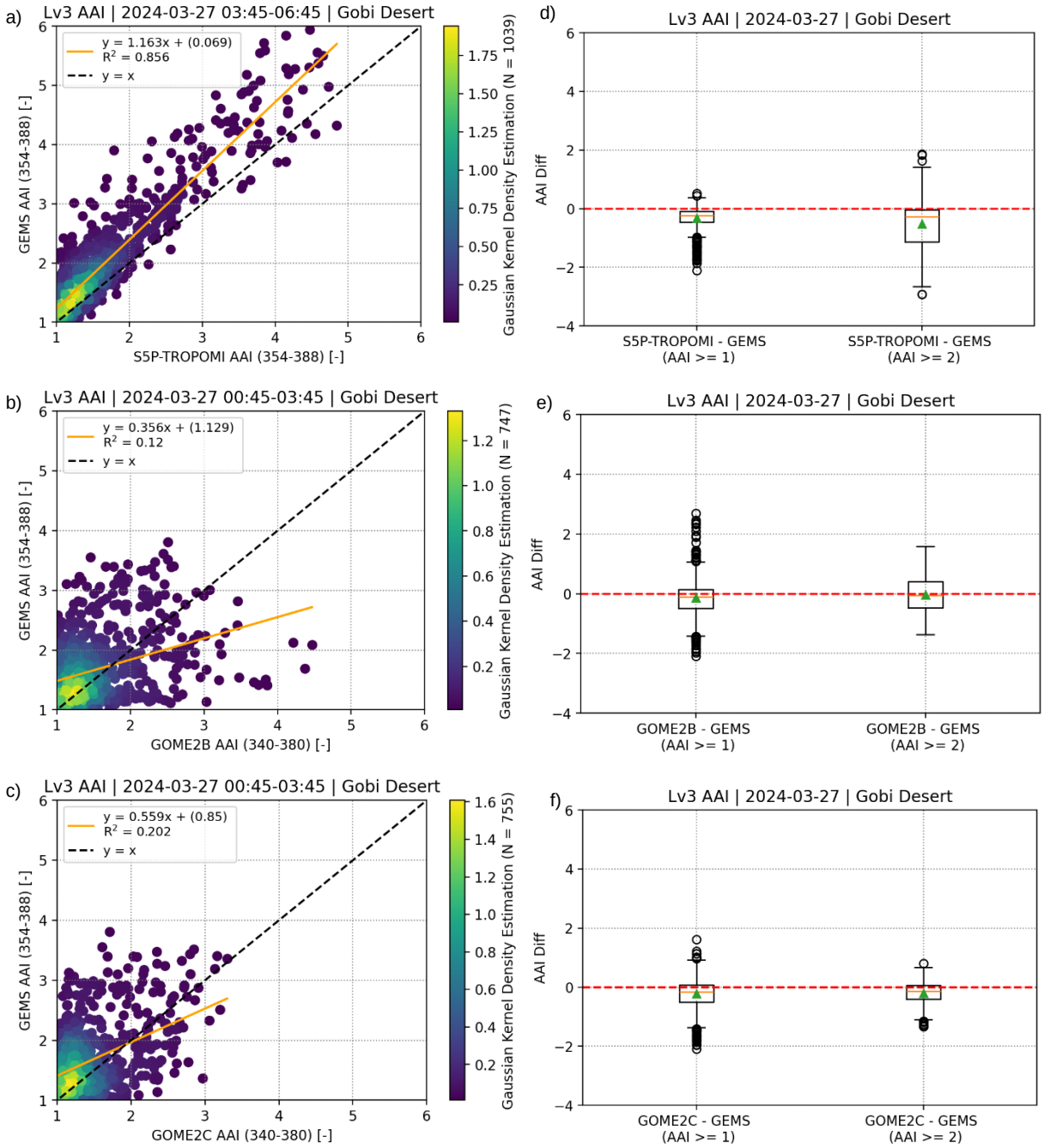

Figure 4-4. Comparisons of the L3 spatiotemporal collocated AAI, for all sensors, on March 27, 2024, as scatter plots (left column) and box plots of the absolute differences between the reference datasets and the GEMS dataset (right column).

Table 4-1. Statistic parameters of the difference distributions, for the case study of March 27, 2024. All differences are between the reference dataset and GEMS, in absolute terms.

Reference dataset	Mean (AAI ≥ 1)	Median (AAI ≥ 1)	Mean (AAI ≥ 2)	Median (AAI ≥ 2)
S5P/TROPOMI	-0.321±0.352	-0.241	-0.521±0.837	-0.28
GOME2B	-0.136±0.634	-0.109	-0.035±0.601	-0.052
GOME2C	-0.222±0.526	-0.156	-0.207±0.442	-0.136

Figure 4-4 presents the results of the comparisons between S5P/TROPOMI – GEMS, GOME-2B – GEMS and GOME-2C – GEMS. In the left column the results are presented as scatter plots, while in the right one the absolute differences between the reference datasets and the GEMS are shown. The results between S5P/TROPOMI and GEMS (panel a) showed a good agreement ($R^2 \approx 0.8$ and slope ≈ 1.2). On the other hand, the results for GOME-2 B&C (panels b and c) were not so good ($R^2 \approx 0.4$-0.5 and slope ≈ 0.2).

In addition, **Table 4-1** presents the statistic results of the box plots in **Figure 4-4** (panels d, e and f). It is apparent that an overestimation of the GEMS AAI was found in all three reference datasets. The mean values of the difference distributions vary from -0.3 to -0.1 for AAI ≥ 1, and from -0.5 to approximately 0 for AAI ≥ 2.

4.3 Case study | April 25, 2024

In this subsection, the results of a case study on April 25, 2024, are presented. The results of the satellite-to-satellite comparisons of the spatiotemporal collocated L3 data are presented below, similarly to subsection **4.2.**

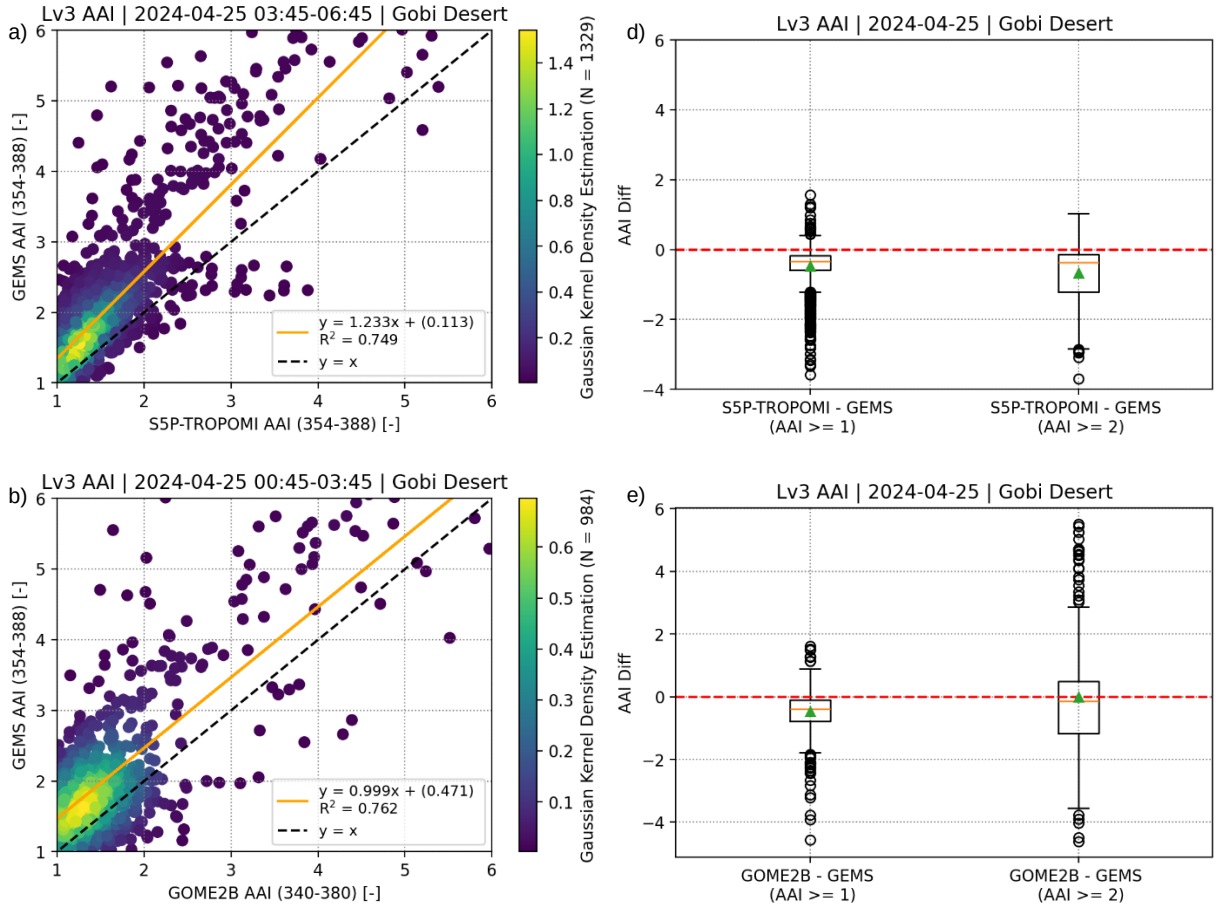

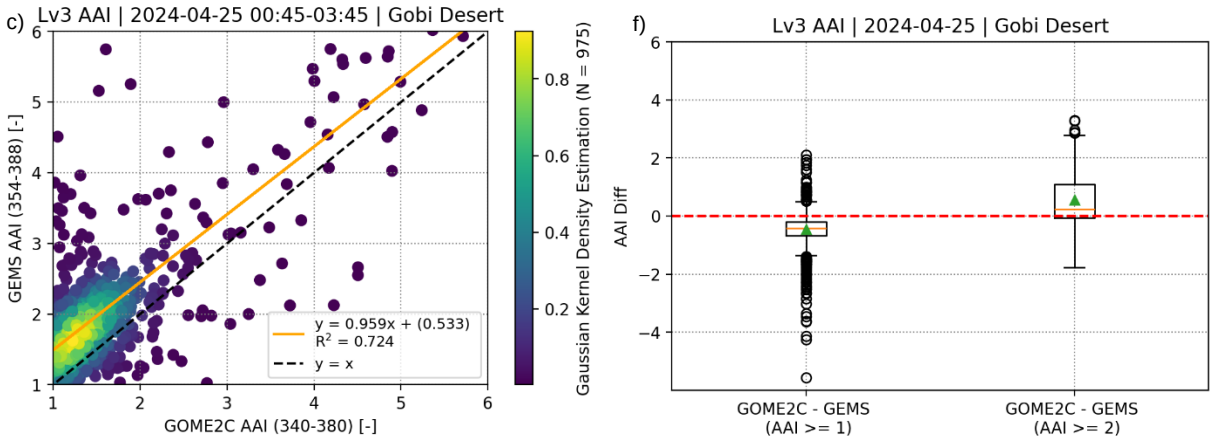

Figure 4-5. Comparisons of the L3 spatiotemporal collocated AAI, for all sensors, on April 25, 2024, as scatter plots (left column) and box plots of the absolute differences between the reference datasets and the GEMS dataset (right column).

Table 4-2. Statistic parameters of the difference distributions, for the case study of April 25, 2024. All differences are between the reference dataset and GEMS, in absolute terms.

Reference dataset	Mean (AAI ≥ 1)	Median (AAI ≥ 1)		Mean (AAI ≥ 2)	Median (AAI ≥ 2)
S5P/TROPOMI	-0.477±0.553	-0.344		-0.675±0.818	-0.365
GOME2B	-0.469±0.623	-0.395		-0.004±2.068	-0.129
GOME2C	-0.467±0.618	-0.422		0.551±1.011	0.246

Figure 4-5 shows the results of the comparisons between S5P/TROPOMI – GEMS, GOME-2B – GEMS and GOME-2C – GEMS as scatter plots (left column) and box plots (right column) of the distributions of the absolute differences between the reference datasets and the GEMS. The results show that in this specific dust event, all three reference datasets (panels a, b, and c) appear to be in a good agreement with the GEMS AAI dataset ($R^2 \approx 0.8$ and slope ≈ 1). However, in this case study, some outliers appear on the comparison results (panels a, b, and c). This shows the effect of the event on the comparison procedure.

Table 4-2 presents the statistic results of the absolute difference distributions in **Figure 4-5** (panels d, e and f). Similar to the previous case study, an overestimation of the GEMS AAI was found, except for the case of GOME-2C, for AAI ≥ 2, where the mean and the median are higher than 0. In general, the mean values of the difference distributions are approximately -0.5 for AAI ≥ 1, for all three reference datasets, and they vary from -0.7 to 0.5 for AAI ≥ 2.

4.4 The effect of the Aerosol Index on the Aerosol Layer Height Evaluation

In this section, we present how the aerosol index may be used to improve the Aerosol Layer Height, ALH, products in space-born observations.

Northeast Asia is affected by various types of aerosols, including dust aerosols produced from the Gobi and Taklamakan deserts and anthropogenic aerosols caused by large regional populations and fossil-fuel combustion processes. A mega dust storm broke out in southeast Mongolia on March 27th, 2021, and significantly impacted air quality in China until March 31st. Dust plumes were first transported to North and Northeast China and the Yellow Sea (March 28th), and then respectively oved eastward to Korea-Japan regions and southward over mainland China (March 29th) resulting in severe degradation of air-quality of mainland China during March 28th to 30th.

We investigated the spatial distribution of GEMS aerosol height for March 28th, 2021. **Figure 4-6**, left, illustrates the corresponding True color satellite image obtained by the MODIS-Terra satellite depicting the transport of the dust plume and cloud coverage over the Eastern Asia during March 28th, 2021. As can be seen, on that day, a distinct, belt-shaped, dense dust plume was visible spread over the Yellow Sea and a significant part of East Asia domain. In addition, HYSPLIT model backward trajectories showed that the dust-containing air masses originated mainly from the Gobi Desert. The UV Aerosol Index (UVAI) and Aerosol Optical Depth (AOD) were also utilized to detect the presence of a high concentration of dust particles in the atmospheric scene. Without the synergistic use of these two indicators, the dust particles could have easily been misidentified as cloud contamination, leading to inaccurate data interpretation.

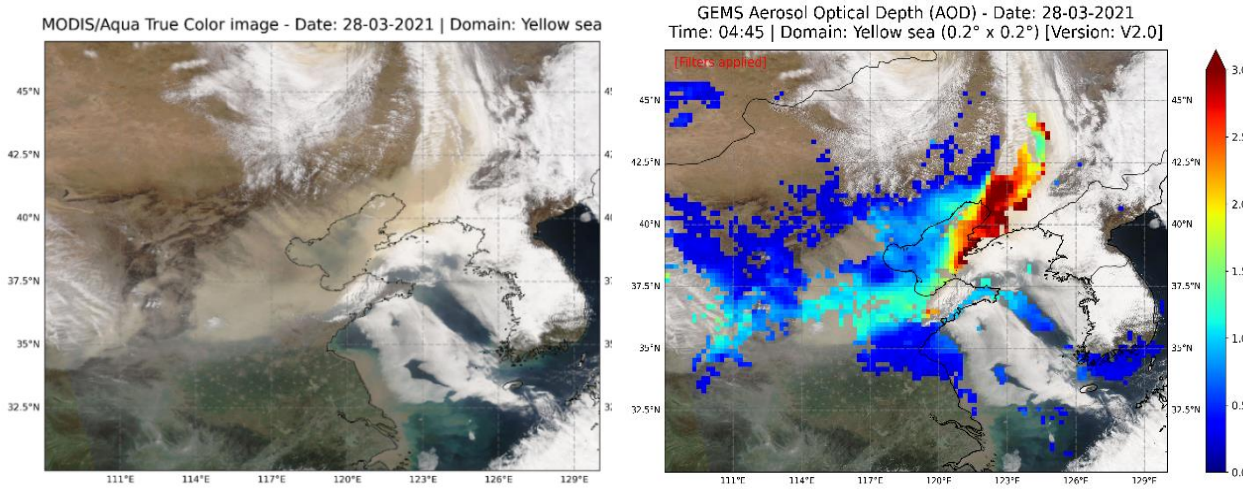

Figure 4-6. (Left) True colour image images captured by MODIS/Terra over E. Asia (Yellow Sea) on March 28,2021. (source: https://worldview.earthdata.nasa.gov/, accessed on August 17,2024) (Right) GEMS L2 Aerosol Optical Depth on March 28th, 2021.

Figure 4-6, right, shows the spatial distribution of gridded (0.2°x0.2°) retrieved pixels obtained by GEMS ALH (AERAOD) operational product, on March 28th, 2021, at 04:45 UTC. On this day, the atmosphere exhibited a substantial presence of highly absorbing aerosol particles. Elevated AOD values exceeding 2.0, as retrieved by the GEMS instrument, indicate a significant aerosol loading and enhancement during the event. The aerosol particle types were characterized using UV and VIS Aerosol Index values provided by the AERAOD algorithm, providing insight into the composition and optical properties of the aerosols.

A satellite-to-satellite comparison between the GEMS against TROPOMI L3 ALH products, for the total number of previously-mentioned cases is presented in the next Figures. For those pixel-to-pixel comparisons, we converted the L2 ALH products into L3 (0.2° x 0.2° gridded data), using the Atmospheric Toolbox HARP package (https://atmospherictoolbox.org/harp, last access October 8, 2024). For the GEMS ALH dataset we used the observational times closer to the S5P-TROPOMI overpasses through the GEMS domain i.e. 03:45, 04:45 and 05:45 UTC. Besides the influence of AOD on the comparisons we furthermore we investigate the performance of the validation status, using stricter criteria regarding the S5P UVAI values: (a) S5P UVAI>0 and (b) S5P UVAI>1.

Figure 4-7 presents the comparison of ALH from GEMS and S5P under two situations: (left) AOD>0.2, S5P UVAI>0 and (Right) AOD>0.4, S5P UVAI>1. As shown in the scatter plots of **Figure 4-7** (upper panel), the performance of GEMS ALH and S5P retrievals is similar, with low correlation with R~0.09 (0.07), a slope of 0.05 (0.07), and an offset 1.534km (1.507km). It is also evident and noted in the graphs, that the number of measurements is significantly reduced (from 37579 to 23539), an aspect which can lead to significant biases. **Figure 4-7** (bottom) shows the absolute differences (GEMS-S5P) of the L3 spatiotemporal collocated ALH products. The near-Gaussian distribution of the absolute difference is centered slightly to the right, indicating higher GEMS ALH values on average with a mean bias of 0.47 km (0.43km) 0.387km (0.091km) and standard deviation of 1.0 km (0.8km) 1.024km (1.086km). Overall, the data show a tendency towards slightly larger values from the GEMS as compared to the TROPOMI data. The application of the criterion for UVAI seems that has a minor effect on the mean bias between the two satellite instruments.

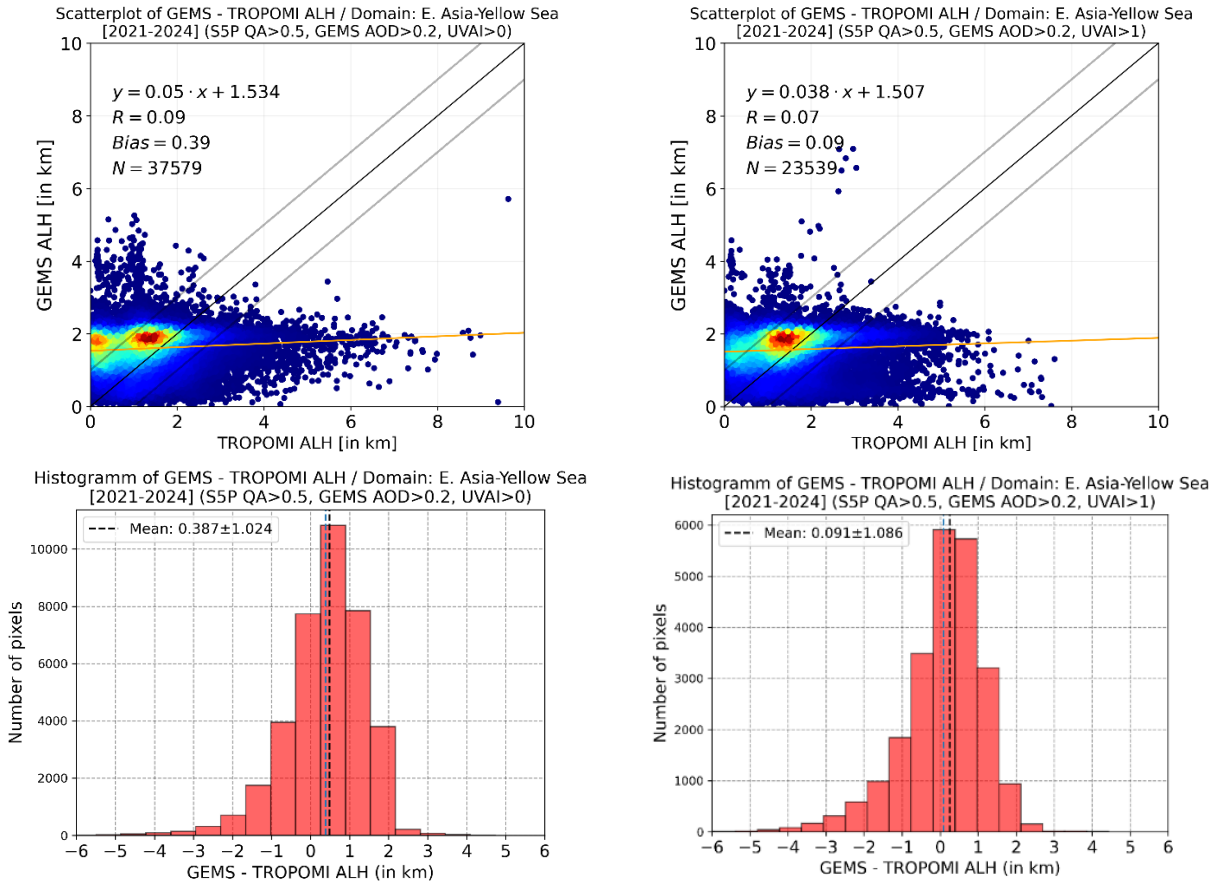

Figure 4-7. (Upper panel) Scatter density plots between the GEMS ALH (y axis) and the inferred TROPOMI ALH (y axis) for period 2021–2023. (bottom panel). Histogram distribution of the absolute differences between difference between GEMS and TROPOMI/S5P ALH collocated gridded data points (left column). Comparisons results where AOD>0.2, UVAI>0 and (right column) where AOD>0.2 and UVAI>1 is applied.

5. Summary and conclusions

To summarize the scientific analysis performed within this VM, we shall employ the consolidated findings based on one of the major dust events over Asia, on March 21st, 2023, part of a larger dust event between the 20th and the 23rd of March 2023 [see section 4.1 and Mikalai et al., 2023)]. This event offered a good agreement in the comparisons with S5P/TROPOMI ($R^2 \approx 0.7$), in contrast to the comparisons against the GOME-2 sensors ($R^2 \approx 0.1$). In Figure 5.1, the distributions of the absolute differences between the L3 reference datasets and GEMS data are presented. In the left column, all types of aerosols identified in the aerosol algorithms are shown, whereas in the right column, only dust aerosols are used for the statistics, as defined in the GEMS data. From top to bottom, comparisons against S5P/TROPOMI, GOME2/MetopB and GOME2/MetopC are shown. Furthermore, in each subfigure, two cases are examined, comparisons where the reported AAI is >= 1 and when AAI > = 2, permitted only the highest events to be included.

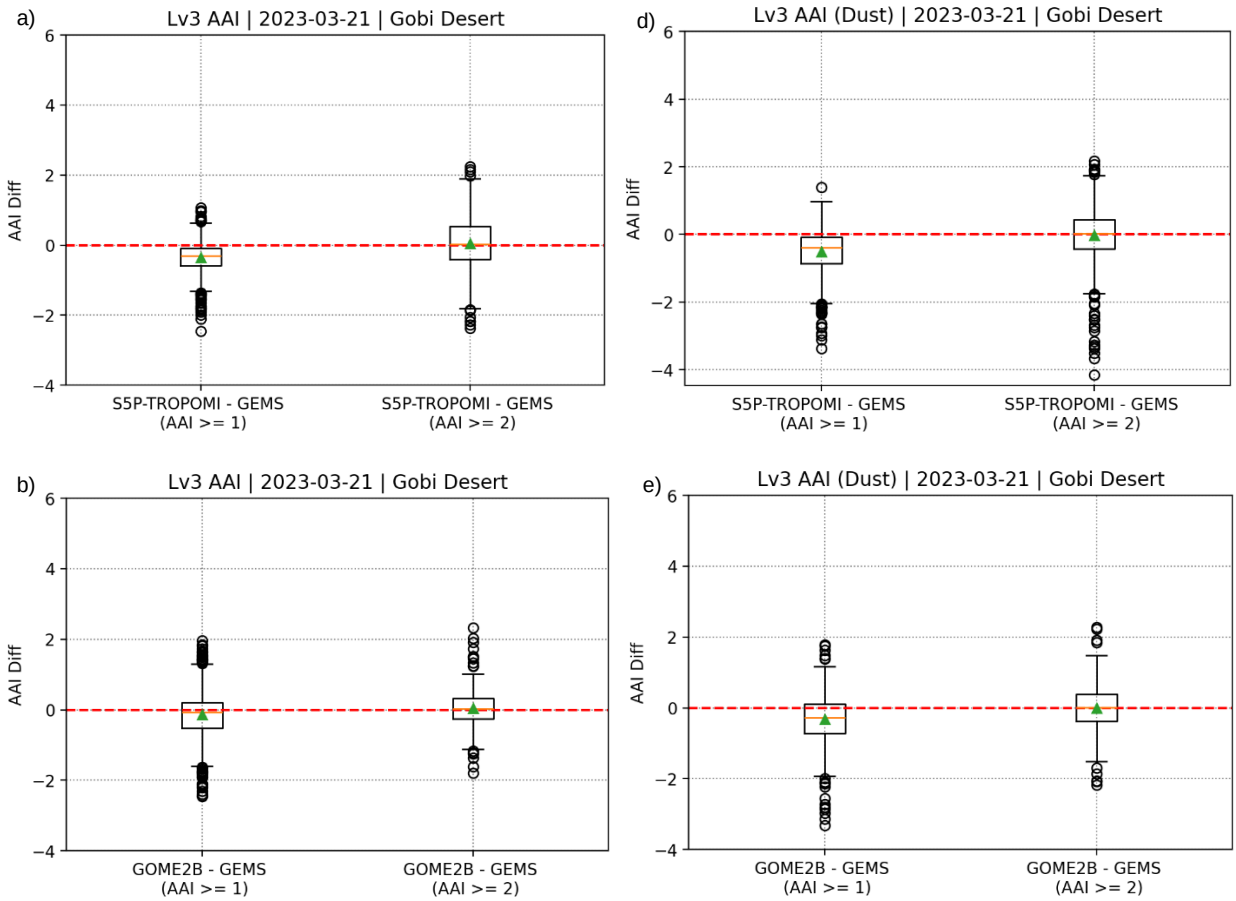

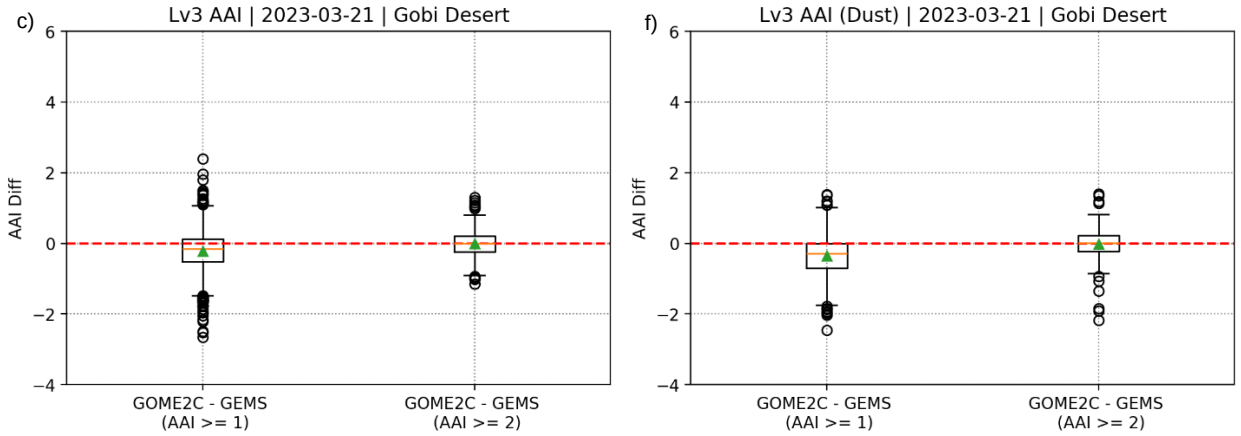

Figure 5-1: Absolute differences of the L3 spatiotemporal collocated AAI, for all sensors, on 21 March 2023, all aerosol types included (left column), only the GEMS dust aerosols included (right column).

Table 5-1: Statistic parameters of the difference distributions, for the case study 21 March 2023. All differences are between the reference dataset and GEMS, in absolute terms.

Reference dataset	Aerosol type	Mean (AAI ≥ 1)	Median (AAI ≥ 1)		Mean (AAI ≥ 2)	Median (AAI ≥ 2)
S5P/TROPOMI	All	-0.349±0.434	-0.3		0.041±0.851	0.033
GOME2B		-0.141±0.68	-0.078		0.046±0.586	0.023
GOME2C		-0.217±0.605	-0.148		-0.009±0.41	-0.004
S5P/TROPOMI	Only Dust	-0.511±0.646	-0.4		-0.035±0.907	0.017
GOME2B		-0.326±0.698	-0.265		-0.007±0.68	0.005
GOME2C		-0.359±0.557	-0.288		-0.019±0.486	0.004

From the results that are presented in both Figure 5.1 and Table 5-1, in the case of AAI ≥ 1, the mean values show a decrease by approximately -0.2, for all sensors, in the case where only the GEMS dust particles are included. The overestimation of the GEMS AAI is also clear, especially in the GEMS only-dust case, however in the case of AAI ≥ 2, the mean values are close to 0, for all sensors, for both the cases where all aerosol types and only the dust particles are included.

These findings are hence covering the HARMONIA COST Action objective *T3.3: Investigate and report on the role of aerosol uncertainty on user requirements*, as the assessment of the different space-born aerosol index products contribute to the assessment of the aerosol layer height uncertainty characterisation, a geophysical parameter of great significance for aerosol related studies. Furthermore, this work significantly contributes to the HARMONIA COST Action deliverable *D3.2 Report on the requirements of different user communities on the accuracy, uncertainty and spatiotemporal resolution of aerosol measurements needed for their activities*.

References

Balis, D., Koukouli, M.-E., Siomos, N., Dimopoulos, S., Mona, L., Pappalardo, G., Marenco, F., Clarisse, L., Ventress, L. J., Carboni, E., Grainger, R. G., Wang, P., Tilstra, G., van der A, R., Theys, N., and Zehner, C.: Validation of ash optical depth and layer height retrieved from passive satellite sensors using EARLINET and airborne lidar data: the case of the Eyjafjallajökull eruption, Atmos. Chem. Phys., 16, 5705–5720, https://doi.org/10.5194/acp-16-5705-2016, 2016.

Chen, S., Bowen Tong, Changzhe Dong, Fu Wang, Binglong Chen, Chonghui Cheng, Xingying Zhang, Dong Liu, Retrievals of aerosol layer height during dust events over the Taklimakan and Gobi desert, Journal of Quantitative Spectroscopy and Radiative Transfer, Volume 254, 2020, https://doi.org/10.1016/j.jqsrt.2020.107198.

Cho, Y., Kim, J., Go, S., Kim, M., Lee, S., Kim, M., Chong, H., Lee, W.-J., Lee, D.-W., Torres, O., and Park, S. S.: First Atmospheric Aerosol Monitoring Results from Geostationary Environment Monitoring Spectrometer (GEMS) over Asia, Atmos. Meas. Tech. Discuss. [preprint], https://doi.org/10.5194/amt-2023-221, in review, 2023.

Go, S.; Kim, J.; Mok, J.; Irie, H.; Yoon, J.; Torres, O.; Krotkov, N.A.; Labow, G.; Kim, M.; Koo, J.-H. Ground-based retrievals of aerosol column absorption in the UV spectral region and their implications for GEMS measurements. Remote Sens. Environ. 2020, 245, 111759.

Griffin, D., Sioris, C., Chen, J., Dickson, N., Kovachik, A., de Graaf, M., Nanda, S., Veefkind, P., Dammers, E., McLinden, C. A., Makar, P., and Akingunola, A.: The 2018 fire season in North America as seen by TROPOMI: aerosol layer height intercomparisons and evaluation of model-derived plume heights, Atmos. Meas. Tech., 13, 1427–1445, https://doi.org/10.5194/amt-13-1427-2020, 2020.

Gui, K., Wenrui Yao, Huizheng Che, Linchang An, Yu Zheng, Lei Li, Hujia Zhao, Lei Zhang, Junting Zhong, Yaqiang Wang, Xiaoye Zhang: Two mega sand and dust storm events over northern China in March 2021: transport processes, historical ranking and meteorological drivers, *Atmospheric Chemistry and Physics*, 2021, https://doi.org/10.5194/acp-2021-933.

Kim, H., Chen, X., Wang, J., Lu, Z., Zhou, M., Carmichael, G., Park, S. S., and Kim, J.: Aerosol layer height (ALH) retrievals from oxygen absorption bands: Intercomparison and validation among different satellite platforms, GEMS, EPIC, and TROPOMI, EGUsphere [preprint], https://doi.org/10.5194/egusphere-2023-3115, 2024.

Kim, J., U. Jeong, M. Ahn, J.H. Kim, R.J. Park, H. Lee, C.H. Song, Y. Choi, K. Lee, J. Yoo, M. Jeong, S.K. Park, K. Lee, C. Song, S. Kim, Y. Kim, S. Kim, M. Kim, S. Go, X. Liu, K. Chance, C. Chan Miller, J. Al-Saadi, B. Veihelmann, P.K. Bhartia, O. Torres, G.G. Abad, D.P. Haffner, D.H. Ko, S.H. Lee, J. Woo, H. Chong, S.S. Park, D. Nicks, W.J. Choi, K. Moon, A. Cho, J. Yoon, S. Kim, H. Hong, K. Lee, H. Lee, S. Lee, M. Choi, P. Veefkind, P. Levelt, D.P. Edwards, M. Kang, M. Eo, J. Bak, K. Baek, H. Kwon, J. Yang, J. Park, K.M. Han, B. Kim, H. Shin, H. Choi, E. Lee, J. Chong, Y. Cha, J. Koo, H. Irie, S. Hayashida, Y. Kasai, Y. Kanaya, C. Liu, J. Lin, J.H. Crawford, G.R. Carmichael, M.J. Newchurch, B.L. Lefer, J.R. Herman, R.J. Swap, A.K. Lau, T.P. Kurosu, G. Jaross, B. Ahlers, M. Dobber, C. McElroy, and Y. Choi: New Era of Air Quality Monitoring from Space: Geostationary Environment Monitoring Spectrometer (GEMS), B. Am. Meteorol. Soc., https://doi.org/10.1175/BAMS-D-18- 0013.1, 2019.00, 2019.

Kim, M.; Kim, J.; Torres, O.; Ahn, C.; Kim, W.; Jeong, U.; Go, S.; Liu, X.; Moon, K.J.; Kim, D.-R. Optimal Estimation-Based Algorithm to Retrieve Aerosol Optical Properties for GEMS Measurements over Asia. Remote Sens. 2018, 10, 162. https://doi.org/10.3390/rs10020162

Michailidis, K., Koukouli, M.-E., Balis, D., Veefkind, P., de Graaf, M., Mona, L., Papagianopoulos, N., Pappalardo, G., Tsikoudi, I., Amiridis, V., Marinou, E., Gialitaki, A., Mamouri, R.-E., Nisantzi, A., Bortoli, D., João Costa, M., Salgueiro, V., Papayannis, A., Mylonaki, M., Alados-Arboledas, L., Romano, S., Perrone, M. R., and Baars, H.: Validation of the TROPOMI/S5P Aerosol Layer Height using EARLINET lidars, Atmos. Chem. Phys. Discuss. [preprint], https://doi.org/10.5194/acp-2022-412, in review, 2022.

Michailidis, K., Koukouli, M.-E., Siomos, N., Balis, D., Tuinder, O., Tilstra, L. G., Mona, L., Pappalardo, G., and Bortoli, D.: First validation of GOME-2/MetOp absorbing aerosol height using EARLINET lidar observations, Atmos. Chem. Phys., 21, 3193–3213, https://doi.org/10.5194/acp-21-3193-2021, 2021.

Mikalai Filonchyk, Michael P. Peterson, Lifeng Zhang, Haowen Yan: An analysis of air pollution associated with the 2023 sand and dust storms over China: Aerosol properties and PM10 variability, Geoscience Frontiers, Volume 15, Issue 2, 2024, 101762, ISSN 1674-9871, https://doi.org/10.1016/j.gsf.2023.101762.

Nanda, S., de Graaf, M., Veefkind, J. P., Sneep, M., ter Linden, M., Sun, J., and Levelt, P. F.: A first comparison of TROPOMI aerosol layer height (ALH) to CALIOP data, Atmos. Meas. Tech., 13, 3043–3059, https://doi.org/10.5194/amt-13-3043-2020, 2020

Sanders, A. F. J., de Haan, J. F., Sneep, M., Apituley, A., Stammes, P., Vieitez, M. O., Tilstra, L. G., Tuinder, O. N. E., Koning, C. E., and Veefkind, J. P.: Evaluation of the operational Aerosol Layer Height retrieval algorithm for Sentinel-5 Precursor: application to O_2 A band observations from GOME-2A, Atmos. Meas. Tech., 8, 4947–4977, https://doi.org/10.5194/amt-8-4947-2015, 2015.

Toth, T. D., Zhang, J., Campbell, J. R., Reid, J. S., and Vaughan, M. A. (2016), Temporal variability of aerosol optical thickness vertical distribution observed from CALIOP, *J. Geophys. Res. Atmos.*, 121, 9117– 9139, doi:10.1002/2015JD024668.

Tuinder, O., de Graaf, M., Tilstra, G., de Vries, M.P. and Kooreman, M.: ATBD for the NRT, Offline and Data Record Absorbing Aerosol Index Products, Doc. No. ACSAF/LNMI/ATBD/002, Issue 2.61, 5 September 2019, KNMI, De Bilt, The Netherlands, 2019.

Veefkind, J.P., Aben, I., McMullan, K., Förster, H., De Vries, J., Otter, G., et al., 2012. TROPOMI on the ESA Sentinel-5 Precursor: a GMES mission for global observations of the atmospheric composition for climate, air quality and ozone layer applications. Remote Sens. Environ. 120, 70–83.

Wang, P., Tuinder, O. N. E., Tilstra, L. G., de Graaf, M. and Stammes, P.: Interpretation of FRESCO cloud retrievals in case of absorbing aerosol events, Atmos. Chem. Phys., 12(19), 9057–9077, doi:10.5194/acp-12-9057-2012, 2012.

Winker, D. M., J. Pelon, J. A. Coakley, Jr., S. A. Ackerman, R. J. Charlson, P. R. Colarco, P. Flamant, Q. Fu, R. M. Hoff, C. Kittaka, T. L. Kubar, H. Le Treut, M. P. Mccormick, G. Mégie, L. Poole, K. Powell, C. Trepte, M. A. Vaughan, and B. A. Wielicki. "The CALIPSO Mission", Bulletin of the American Meteorological Society 91, 9 (2010): 1211-1230, https://doi.org/10.1175/2010BAMS3009.1.

Winker, D. M., Tackett, J. L., Getzewich, B. J., Liu, Z., Vaughan, M. A., and Rogers, R. R.: The global 3-D distribution of tropospheric aerosols as characterized by CALIOP, Atmos. Chem. Phys., 13, 3345–3361, https://doi.org/10.5194/acp-13-3345-2013, 2013.